

Supplemental Data

Material and Methods

Preparation of serum and mesenchymal stem cells from rats

Serum was prepared from tMCAo rat stroke animal models (RSS) and normal rats (RNS). The blood was collected by cardiac puncture, from the still-beating heart, with a 5-mL syringe.

Rat MSCs (rMSCs) were obtained from femora and tibias of Sprague Dawley rats (male, weighing 220–250 g, n=10–13), as previously described¹.

The rMSCs were characterized by flow cytometry analysis, and their expression levels of CD90, CD29 (positive surface marker, BD Biosciences), CD45, and CD11b (negative surface marker, BD Biosciences) were evaluated by flow cytometry (FACS Calibur; BD Biosciences).

Real-time quantitative PCR for rat trophic factors

Total RNA was extracted using Trizol™ (GIBCO). cDNA was synthesized from 2 µg of total RNA using oligo d(T)₁₆ primers and the Omniscript RT-kit (Qiagen). For quantitative real-time PCR analysis of *VEGF*, *GDNF*, *FGF2*, and *GAPDH*, TaqMan assays were performed using TaqMan gene expression Master Mix (Thermo Fisher Scientific) on an ABI Prism 7900 Real-time PCR system (Applied Biosystems). Primers and probes were obtained commercially (Thermo Fisher Scientific) and are described in Table S1.

Cell cycle analysis

Cells were collected and fixed with ice-cold 90% ethanol that was added dropwise during vortexing. The fixation reaction was allowed to proceed for 1–24 hours while the cells were kept at 4°C. Cells were then collected by centrifugation, re-suspended in phosphate buffered saline (PBS) containing 0.1% Triton X-100 and 20 µg/mL RNase, and incubated for 30 minutes at 37°C. Propidium iodide was added to a final concentration of 50 µg/mL, and cells were analyzed by flow cytometry. To measure cell cycle distribution, 10,000 MSCs were obtained with Cell Quest software and analyzed with Modfit software². The length of the G₀/G₁ phase was calculated using the following equation: $T_{(G_0/G_1)} = [T_{(C)} \times \ln(F_{(G_0/G_1)} + 1)] / \ln 2$, where

$T_{(G0/G1)}$ and $T_{(C)}$ are the duration of the G0/G1 phase and the doubling time, respectively, and $F_{(G0/G1)}$ is the percentage of cells in the G0/G1 phase³.

Analysis of cell death

For FCM analysis to determine cell death, rMSCs were stained with Annexin V-FITC (BD Biosciences) and propidium iodide (PI, Sigma), following the manufacturer's staining protocol. Briefly, 100 μ L of cell suspension (1×10^5 cells in 1X binding buffer) were stained with 2.5 μ L of Annexin V-FITC and 5 μ L of PI (50 μ g/mL), mixed gently, and incubated for 15 min at room temperature in the dark, following which 200 μ L of 1X Annexin binding buffer were added and the cells were immediately analyzed by flow cytometry. FCM analysis was performed using a FACS Calibur flow cytometer. Data for 10,000 cells were collected at a low flow rate and analyzed using CellQuest software (BD Biosciences). The Annexin V-FITC signal was detected using an FL1 detector and PI was detected by an FL2 detector. Discrimination between living, necrotic, and apoptotic cells was based on changes in the phosphatidylserine asymmetry of the cell membrane, as detected by Annexin V binding. Analyses of the cell death process using simultaneous staining with FITC-Annexin V (green fluorescence) and non-vital dye PI (red fluorescence) allowed the discrimination between intact cells (FITC⁻/PI⁻), early apoptotic cells (FITC⁺/PI⁻), and late apoptotic or necrotic cells (FITC⁺/PI⁺).

Results

Phenotypic characterization of MSCs

The phenotypic characteristics of rMSCs were compared after they had been cultured using different media; BM-MSCs were expanded in 10% FBS, 10% RNS, or 10% RSS. The morphology of rMSCs did not differ between groups (Fig. S2A). rMSCs cultured with RNS or RSS had a significantly higher cumulative population doubling level (CPDL) compared with those cultured in FBS (Fig. S2B, ** $p < 0.01$). All rMSCs were CD90-, CD73-positive ($\geq 95\%$ positive) and CD34-, CD45-negative ($\leq 1\%$ positive) (Fig. S2C).

To compare whether RSS improves trophic factor gene expression levels, rMSCs were cultured with various serum sources. rMSCs cultured with RSS (RSS-rMSCs) showed significantly

greater expression of VEGF and FGF2 than BM-MSCs cultured with FBS (FBS-rMSCs) or RNS (RNS-rMSCs) (Fig. S2D, F, ** $p < 0.01$). GDNF was significantly more greatly expressed in RSS-rMSCs than in FBS-rMSCs (Fig. S2E, ** $p < 0.01$).

Proliferative capacity of rMSCs

To compare the proliferative capacities of RSS-rMSCs collected at different time points after stroke, rMSCs were cultured for passages 2–4. FBS-rMSCs showed the lowest population doubling level (Fig. S3A). The CPDL at P4 of RSS-rMSCs (mean \pm SEM, 1 d 2.70 \pm 0.03, 7 d 2.84 \pm 0.01, 14 d 2.88 \pm 0.04, 28 d 2.84 \pm 0.03, 60 d 2.53 \pm 0.03, 90 d 2.53 \pm 0.03) was significantly higher than those of FBS-rMSCs (mean \pm SEM, 1.63 \pm 0.12) or RNS-rMSCs (mean \pm SEM, 2.17 \pm 0.02) (* $p < 0.05$, ** $p < 0.01$, respectively). Population doubling times (PDTs) of RNS-rMSCs and RSS-rMSCs remained at low levels, but increased with the passage number of the FBS-rMSCs. The PDT of FBS-rMSCs increased with culture expansion; the PDT of FBS-rMSCs was around 60 h at P2, and increased to 88 h by P4. In contrast, the PDT of RSS-rMSCs retained a short doubling time of 31–45 h. Similar results were obtained for RNS-rMSCs (approximately 43–62 h) (Fig. S3B, * $p < 0.05$, ** $p < 0.01$).

Cell cycle analyses using FCM analysis showed different distributions in the cell cycle, depending on the serum source. Specifically, a greater population of cells that were cultured with RSS occupied the proliferating phase of the cell cycle at P3 (S/G2-M phase) compared with FBS- rMSCs or RNS-rMSCs (Fig. S3C, * $p < 0.05$, ** $p < 0.01$), except in the RSS culture after 28 d ($p = 0.065$). Based on PDT and cell cycle distribution, we calculated the duration of G0/G1. The average duration of the G0/G1 phase in FBS-rMSCs increased from approximately 53 h at P2 to 77 h at P4. Notably, a shortening of the duration of the G0/G1 phase was observed in cells cultured with RSS in consecutive divisions (with a range of 26–37 h, Fig. S3D, * $p < 0.01$).

Survival and cellular senescence of MSCs

To examine whether RSS improves the survival of rMSCs under toxic ischemic brain conditions, rMSCs were treated with ischemic brain-conditioned media, including 20% IBE, after which cell viability was measured. FCM analysis showed that fewer apoptotic cells (Annexin V positive) and necrotic cells (PI positive) were observed among RSS-rMSCs, compared to FBS-rMSCs or RNS-rMSCs (Fig. S4A). The effects of the RSS on MSC survival

in ischemic brain conditions were more prominent when rMSCs were cultured with serum obtained at 1 day after tMCAo (Fig. S4B, * $p < 0.01$).

In addition, the effect of RSS on cellular senescence was evaluated using SA- β -gal staining, a senescence marker (Fig. S4C). Approximately 42% of rMSCs cultured with FBS revealed senescence-associated changes at P6. The proportion of SA- β -gal-positive cells was significantly lower among RNS- rMSCs or RSS-rMSCs than among FBS-rMSCs (Fig. S4D, * $p < 0.01$).

Our data show that culture expansion using RSS enhances rMSC survival under toxic ischemic conditions. One of the limiting factors is poor local survival of transplanted stem cells. Only a few transplanted MSCs and newly formed neurons in the infarcted hemisphere died within several weeks^{1, 4, 5}. Poor vascular and microenvironmental conditions, including increased tissue levels of free radicals, excitotoxic neurotransmitters, and proinflammatory cytokines, might threaten transplanted cells migrating into the peri-infarct region. In addition, MSCs provide trophic support to the ischemic brain, which can be enhanced by ex vivo administration of trophic factors⁶ or preconditioning during the cultivation of MSCs^{7, 8}.

hMSC culture

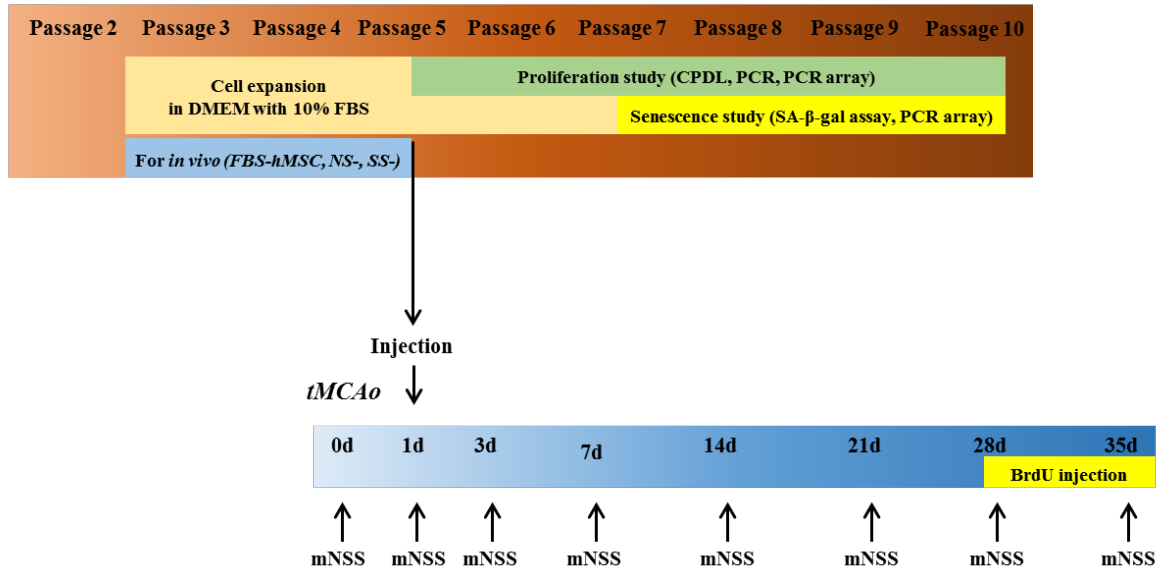


Figure 1. *Experimental time line*

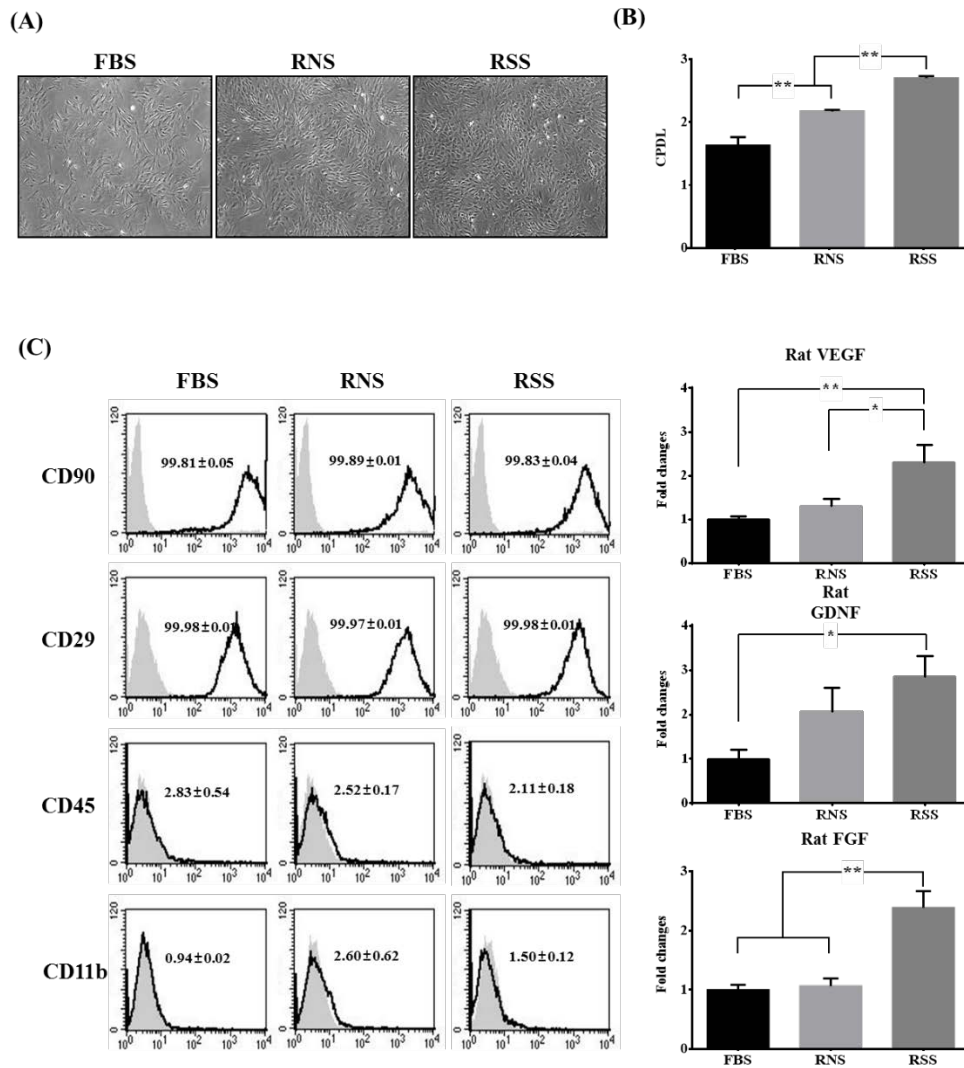


Figure 2. Evaluation of phenotypic characteristics of MSCs

Representative phase contrast images of rMSCs expanded with the different types of serum. (B) PDL of rMSCs cultured with FBS, RNS, and RSS. (C) FACS analysis of rMSCs cultured with different types of serum. Quantitative analysis of the percentages of cells expressing CD90, CD29 (positive markers), and CD45, CD11b (negative markers). The relative expression levels of both (D) rat VEGF and (E) rat GDNF were significantly higher in rMSCs cultured with allogeneic serum culture (RNS, RSS) than with FBS. (F) The relative expression level of rat FGF was significantly higher in RSS- than in FBS or RNS. Data are presented as mean \pm SEM (* $p < 0.05$, ** $p < 0.01$, $n = 4 \sim 6$).

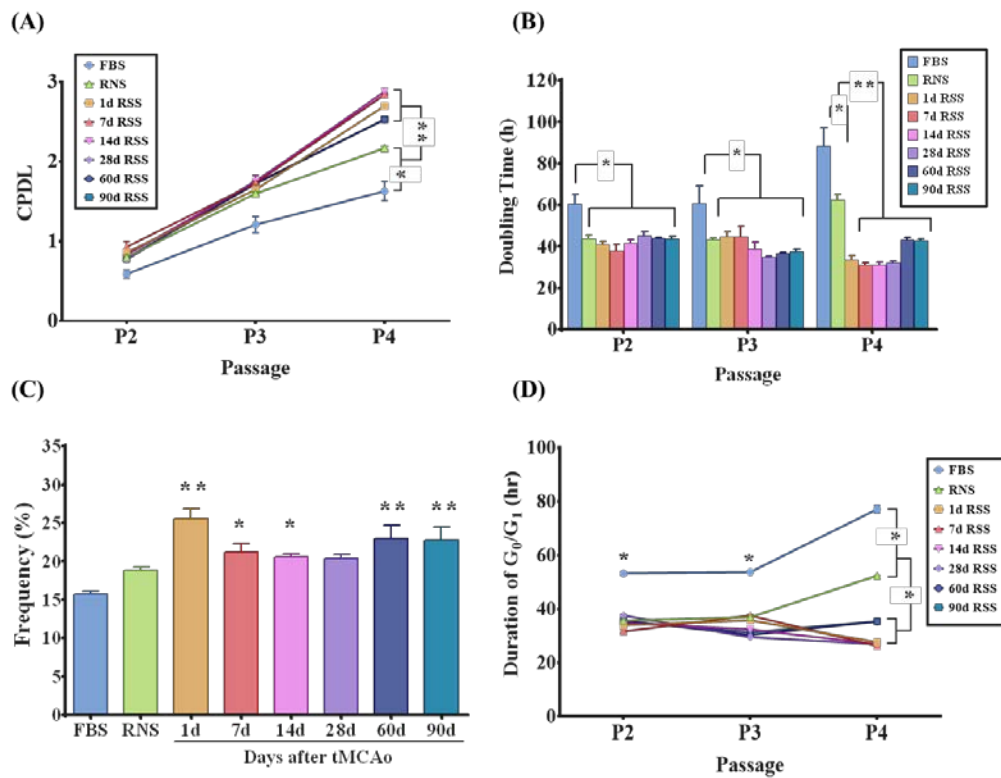


Figure 3. Proliferative properties of rMSCs cultured with different types of serum from P2 to P4.

(A) Cumulative population doubling levels (CPDLs) were determined in different types of serum. (B) Cell doubling time was calculated for rMSCs cultured with FBS, RNS, and RSS (1, 7, 14, 28, 60, and 90 days after tMCAo). (C) A comparison of proliferative phase frequency (S phase + G2/M phase) of rMSCs cultured with different serum at P3. (D) Calculation of G0/G1 phase length from population number and cell cycle data from P2-4. Results are presented as mean±SEM (* $p < 0.05$, ** $p < 0.01$, $n = 4 \sim 6$).

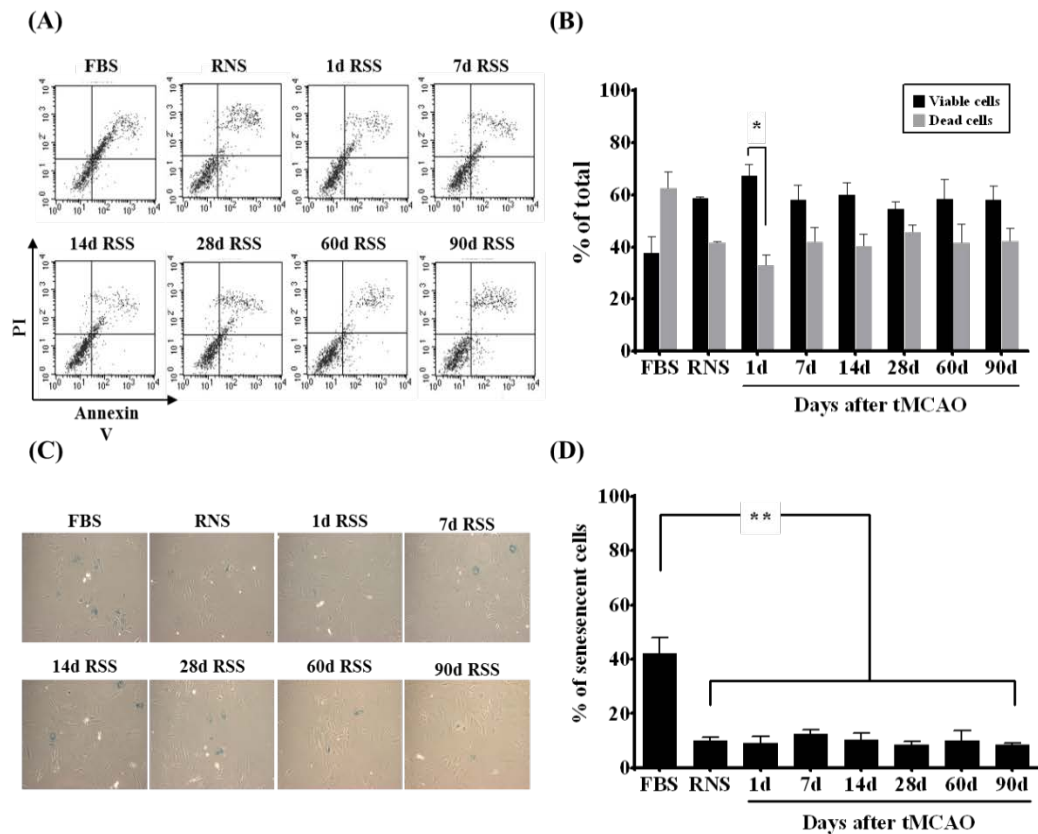


Figure 4. Cell viability in ischemic brain conditions and senescence of rMSCs

rMSCs cultured with FBS, RNS, or RSS (1, 7, 14, 28, 60, and 90 days after stroke) were exposed to 20% IBE for 24 h at P4. (A) Representative scatter plots showing the distributions of Annexin V and PI staining. Cells are classified as “viable” (bottom left), “apoptotic” (bottom right), or “necrotic” (top left and right). (B) Quantitative analysis of cell viability, presented as the percentage of viable and dead (apoptotic+necrotic) cells at P4 by FCM analysis. The data are presented as mean±SEM (* *p*<0.05, n=4~6). (C) rMSCs were stained with β-galactosidase staining solution. Representative images of SA-β-Gal staining. (D) Quantitative analysis of senescence, expressed as the percentage of positively stained cells at P6. The absolute number of blue stained cells was counted in 6 fields per well. The data are presented as mean±SEM (** *p*<0.01, n=3).

Table 1. PCR primer for Real-time qPCR

Gene	Product Name	
	Rat	Human
<i>VEGF</i>	<i>Rn01511605_m1</i>	<i>P128356</i>
<i>GDNF</i>	<i>Rn00569510_m1</i>	<i>P171077</i>
<i>FGF2</i>	<i>Rn00570809_m1</i>	<i>P111196</i>
<i>GAPDH</i>	<i>4352338E</i>	<i>P267613</i>

Table 2. List of differentially expressed serum proteins ($p < 0.05$) between healthy subjects and stroke patients

No	Proteins	Stroke/Normal		UniProt
		Fold change	p-value	
1	Activin C	1.503	0.037	P36896
2	Activin RIA	1.696	0.015	Q13705
3	Activin RIB	2.081	0.014	P27037
4	Activin RII A/B	1.558	0.006	Q15848
5	Angiogenin	1.802	0.021	O15123
6	Angiopoietin-1	1.712	0.008	Q9Y264
7	Amphiregulin	1.693	0.002	P30530
8	Artemin	1.897	0.006	P33681
9	BDNF	1.875	0.013	Q07812
10	CXCL13	1.686	0.011	P12645
11	BMP-5	1.803	0.029	P18075
12	BMP-8	1.713	0.008	P36894
13	BMP-15	1.805	0.012	O00238
14	BMPR-IB	2.303	0.006	P35070
15	BTC	1.638	0.029	Q16627
16	CCL14	2.138	0.027	P32246
17	CCR7	4.252	0.026	P51686
18	CD40L	2.368	0.045	O95813
19	CRIM 1	2.147	0.034	Q9Y5Y4
20	Cripto-1	2.737	0.047	Q9GZR3
21	CD152	1.855	0.012	O95715
22	Crossveinless-2	1.580	0.039	Q9H2A7
23	CXCR6	2.482	0.015	P41271
24	DANCE	1.878	0.017	P07585
25	DcR3	1.795	0.041	O94907

26	Dkk-4	1.628	0.019	O75509
27	EGF	1.868	0.007	P58294
28	EMAP-II	2.063	0.007	Q9NQ30
29	CD105	1.566	0.018	P05305
30	CCL26	2.282	0.047	P04626
31	Epiregulin	1.785	0.008	P21860
32	ErbB3	2.250	0.031	P01588
33	ErbB4	2.169	0.007	P16581
34	E-Selectin	1.909	0.036	P58499
35	Fas Ligand	2.603	0.028	Q14512
36	FGF Basic	2.312	0.038	P22607
37	FGF-BP	1.648	0.010	P22455
38	FGF-5	2.145	0.014	P21781
39	FGF-12	1.783	0.013	O43320
40	FGF-23	1.675	0.030	P36888
41	Flt-3 Ligand	2.608	0.008	Q12841
42	Frizzled-1	1.651	0.042	Q9ULV1
43	Frizzled-4	1.997	0.005	O60353
44	Galectin-3	2.112	0.013	Q96NZ8
45	GASP-2	1.650	0.039	P09919
46	Glut1	1.815	0.029	P11169
47	Glypican 5	1.704	0.007	P15509
48	Granzyme A	1.756	0.040	P12544
49	Growth Hormone	1.948	0.024	Q99075
50	CRAM-A/B	1.972	0.001	Q04760
51	Hepassocin	2.031	0.004	P14210
52	IFN- γ R1	1.968	0.045	P18065
53	IGF-II	2.332	0.004	P01583
54	IL-1F10	1.659	0.042	Q01638
55	IL-1 sRII	1.696	0.013	P01589
56	IL-2R β	1.601	0.036	P08700
57	IL-12 p40	1.519	0.034	P42701
58	IL-12 p70	1.563	0.022	Q99665
59	IL-15R α	1.892	0.027	Q16552
60	IL-17	2.300	0.030	Q9NRM6
61	IL-17D	1.815	0.020	Q96PD4
62	IL-20	2.099	0.035	Q6UXL0
63	Kininostatin	1.872	0.032	Q8NCW0
64	Kremen-1	2.061	0.015	P22064
65	Latent TGF- β bp1	1.562	0.021	P06239

66	Lipocalin-2	3.520	0.011	O75581
67	MCP-1	1.778	0.016	P80098
68	MFRP	1.742	0.028	P14174
69	MIG	2.299	0.045	P13236
70	MIP-1 α	1.772	0.010	Q16663
71	MMP-9	3.125	0.010	P24347
72	OSM	1.956	0.019	P61366
73	Osteoprotegerin	2.217	0.049	P55774
74	P-selectin	1.927	0.019	Q9Y6Q6
75	RAGE	1.874	0.014	P13501
76	ROBO4	1.975	0.023	P60903
77	S100 A8/A9	3.171	0.016	P0DJI8
78	sgp130	1.828	0.023	O15389
79	Soggy-1	1.535	0.048	P09486
80	Spinesin	1.771	0.031	Q92583
81	TLR1	1.830	0.028	O15455
82	Tomoregulin-1	2.124	0.011	P01375
83	TNF- β	1.945	0.020	P20333
84	TRADD	2.959	0.009	O00220
85	TRAIL R2	2.061	0.041	Q9UBN6
86	TSG-6	1.776	0.021	O43508
87	VEGF	2.065	0.038	P35916
88	VEGF-D	1.796	0.026	Q9Y5W5

Table S3. List of differentially expressed paracrine proteins ($p < 0.05$) between healthy subjects and stroke patients

No	Proteins	Stroke/Normal		UniProt
		Fold change	p-value	
1	Activin A	3.95	0.045	P08476
2	Artemin	2.43	0.034	Q5T4W7
3	BMP-2	1.66	0.042	P12643
4	CCN3	1.82	0.003	P48745
5	Cerberus 1	1.99	0.006	O95813
6	CTGF	1.91	0.027	P29279
7	CXCL7	2.41	0.049	P02775
8	EDA2R	1.94	0.007	Q9HAV5
9	FACX	1.84	0.037	P00742
10	FGF-11	1.74	0.038	Q92914

11	Fractalkine	2.30	0.023	P78423
12	GFR alpha-1	1.64	0.049	P56159
13	Grb2	2.00	0.027	P62993
14	IGFBP-1	2.14	0.051	P08833
15	IGFBP-4	1.78	0.035	P22692
16	IGFBP-6	1.76	0.016	P24592
17	IL-1 R3	1.83	0.009	Q9NPH3
18	IL-12 R beta 2	1.60	0.013	Q99665
19	IL-15 R alpha	2.55	0.012	Q13261
20	IL-17B	2.98	0.042	Q9UHF5
21	IL-17F	1.85	0.032	Q96PD4
22	IL-21 R	1.92	0.039	Q9HBE5
23	IL-24	1.92	0.005	Q13007
24	IL-31 RA	1.90	0.017	Q8NI17
25	IL-36G	1.94	0.002	Q9NZH8
26	Kininostatin	3.70	0.010	P01042
27	LECT2	2.02	0.031	O14960
28	Lep	1.85	0.002	P41159
29	LIF	1.66	0.039	P15018
30	LRP-1	2.50	0.041	Q07954
31	Lymphotoxin beta R	1.83	0.025	P36941
32	MAC-1	1.69	0.043	P11215
33	MCP-1	1.91	0.051	P13500
34	MIP-1delta	1.79	0.017	Q16663
35	MIP-2	1.85	0.026	P19875
36	MIP-3 alpha	2.00	0.045	P78556
37	MIP-3 beta	1.87	0.017	Q99731
38	MMP-13	1.64	0.002	P45452
39	MMP-14	1.51	0.019	P50281
40	MMP-16	1.58	0.006	P51512
41	MMP-3	1.89	0.006	P08254
42	MMP-7	1.76	0.007	P09237
43	Neurturin	1.60	0.013	Q99748
44	NGF R	1.87	0.042	P08138
45	Nidogen-1	1.82	0.009	P14543
46	Neurotrophin-4	2.53	0.040	P34130
47	Orexin A	2.40	0.042	O43612
48	Osteoprotegerin	2.07	0.049	O00300
49	OX40 Ligand	1.85	0.025	P23510
50	PD-ECGF	1.53	0.007	P19971

51	PDGF R beta	1.66	0.027	P09619
52	PDGF-AA	2.09	0.022	P04085
53	PDGF-BB	2.60	0.047	P01127
54	PDGF-C	2.00	0.029	Q9NRA1
55	Peroxiredoxin 6 (Prdx6)	2.04	0.012	P30041
56	PLUNC	1.89	0.004	Q9NP55
57	Prolactin	1.53	0.027	P01236
58	P-selectin	1.58	0.023	P16109
59	RAGE	2.09	0.007	Q15109
60	RELM beta	2.28	0.036	Q9BQ08
61	S100 A8/A9	2.31	0.050	P05109, P06702
62	Secreted frizzled-related protein 1	1.93	0.007	Q8N474
63	Secreted frizzled-related protein 4	1.97	0.012	Q6FHJ7
64	sFRP-3	2.90	0.043	Q92765
65	Sonic Hedgehog (Shh N-terminal)	2.54	0.019	Q15465
66	TGF-beta RII	2.02	0.047	P37173
67	TGF-beta RIII	1.70	0.033	Q03167
68	Thrombopoietin (TPO)	1.79	0.001	P40225
69	Thyroid Peroxidase	1.67	0.003	P07202
70	TIMP-2	4.85	0.009	P16035
71	TL1A / TNFSF15	1.72	0.022	O95150
72	TLR1	1.76	0.024	Q15399
73	TLR2	1.89	0.031	O60603
74	TLR3	1.75	0.015	O15455
75	TMPRSS5	1.83	0.021	Q9H3S3
76	TRADD	1.54	0.022	Q15628
77	TRAIL R3	2.03	0.027	O14798
78	TRAIL R4	1.79	0.040	Q9UBN6
79	TRAIL	2.36	0.028	P50591
80	TROY	1.57	0.012	Q9NS68
81	Vasorin	1.65	0.031	Q6EMK4
82	VCAM-1	2.00	0.002	P19320
83	VE-Cadherin	1.82	0.037	P33151
84	KDR	1.93	0.011	P35968
85	VEGF R3	1.95	0.005	P35916
86	VEGFA	1.97	0.018	P15692

Table 4. Checklist of Methodological and Reporting Aspects

Methodological and Reporting Aspects	Description of Procedures
Experimental groups and study timeline	<ul style="list-style-type: none"> ☒ The experimental group(s) have been clearly defined in the article, including number of animals in each experimental arm of the study. ☒ An account of the control group is provided, and number of animals in the control group has been reported. If no controls were used, the rationale has been stated. ☒ An overall study timeline is provided. (supplementary figure)
Inclusion and exclusion criteria	<ul style="list-style-type: none"> ☒ A priori inclusion and exclusion criteria for tested animals were defined and have been reported in the article.
Randomization	<ul style="list-style-type: none"> ☒ Animals were randomly assigned to the experimental groups. If the work being submitted does not contain multiple experimental groups, or if random assignment was not used, adequate explanations have been provided. ☒ Type and methods of randomization have been described. ☒ Methods used for allocation concealment have been reported.
Blinding	<ul style="list-style-type: none"> ☒ Blinding procedures have been described with regard to masking of group/treatment assignment from the experimenter. The rationale for nonblinding of the experimenter has been provided, if such was not feasible. ☒ Blinding procedures have been described with regard to masking of group assignment during outcome assessment.
Sample size and power calculations	<ul style="list-style-type: none"> ☒ Formal sample size and power calculations were conducted based on a priori determined outcome(s) and treatment effect, and the data have been reported. OR A formal size assessment was not conducted and a rationale has been provided.
Data reporting and statistical methods	<ul style="list-style-type: none"> ☒ Number of animals in each group: randomized, tested, lost to follow-up, or died have been reported. If the experimentation involves repeated measurements, the number of animals assessed at each time point is provided, for all experimental groups. ☒ Baseline data on assessed outcome(s) for all experimental groups have been reported. ☒ Details on important adverse events and death of animals during the course of experimentation have been provided, for all experimental arms. ☒ Statistical methods used have been reported. ☒ Numeric data on outcomes have been provided in text, or in a tabular format with the main article or as supplementary tables, in addition to the figures.

Experimental details, ethics, and funding statements	<ul style="list-style-type: none"><input checked="" type="checkbox"/> Details on experimentation including stroke model, formulation and dosage of therapeutic agent, site and route of administration, use of anesthesia and analgesia, temperature control during experimentation, and postprocedural monitoring have been described.<input checked="" type="checkbox"/> Different sex animals have been used. If not, the reason/justification is provided.<input checked="" type="checkbox"/> Statements on approval by ethics boards and ethical conduct of studies have been provided.<input checked="" type="checkbox"/> Statements on funding and conflicts of interests have been provided.
--	---

References

- 1 Li WY, Choi YJ, Lee PH *et al.* Mesenchymal stem cells for ischemic stroke: changes in effects after ex vivo culturing. *Cell Transplant* 2008; **17**:1045-1059.
- 2 Rosova I, Dao M, Capoccia B, Link D, Nolte JA. Hypoxic preconditioning results in increased motility and improved therapeutic potential of human mesenchymal stem cells. *Stem Cells* 2008; **26**:2173-2182.
- 3 Pozarowski P, Darzynkiewicz Z. Analysis of cell cycle by flow cytometry. *Methods in molecular biology* 2004; **281**:301-311.
- 4 Borlongan CV, Kaneko Y, Maki M *et al.* Menstrual blood cells display stem cell-like phenotypic markers and exert neuroprotection following transplantation in experimental stroke. *Stem cells and development* 2010; **19**:439-452.
- 5 Nadareishvili Z, Hallenbeck J. Neuronal regeneration after stroke. *The New England journal of medicine* 2003; **348**:2355-2356.
- 6 Choi YJ, Li WY, Moon GJ *et al.* Enhancing trophic support of mesenchymal stem cells by ex vivo treatment with trophic factors. *J Neurol Sci* 2010; **298**:28-34.
- 7 Wang JA, He A, Hu X *et al.* Anoxic preconditioning: a way to enhance the cardioprotection of mesenchymal stem cells. *International journal of cardiology* 2009; **133**:410-412.
- 8 Pasha Z, Wang Y, Sheikh R, Zhang D, Zhao T, Ashraf M. Preconditioning enhances cell survival and differentiation of stem cells during transplantation in infarcted myocardium. *Cardiovasc Res* 2008; **77**:134-142.